Combined Thermofluid and Electromagnetic Optimisation of Stator Vent Cooling

K. Bersch, S. Nuzzo, P.H. Connor, C.N. Eastwick, M. Galea, R. Rolston, G. Vakil

Abstract – **A combined electromagnetic and thermal modelling approach has been developed to optimise the design of multiple radial stator vents in an air-cooled, synchronous generator with a power rating of several hundred kVA. An experimentally validated 3-D Conjugate Heat Transfer Computational Fluid Dynamics model has been created and coupled with 2-D Electromagnetic Finite Element Analysis. Correlations between the combined vent width and rotor copper, rotor iron and stator iron losses were derived from the electromagnetic analysis. These correlations were implemented into the optimisation procedure of the parametric thermofluid model. Five parameters: vent locations, widths and the height of a baffle, were optimised simultaneously with the aim of minimising the peak stator winding temperature. The peak stator winding temperature was reduced by 11.1 %. The average stator winding temperature decreased by 6.3 %. To maintain the machine's power output, the removal of active stator material was compensated by increasing the rotor current.**

Index Terms— **Alternators, cooling, electric machines, electromagnetic modelling, energy efficiency, fluid dynamics, generators, magnetic losses, thermal management**

I. INTRODUCTION

WITHIN this paper, a synchronous generator with a power rating of several hundred kVA has been analysed using a multi-physics approach to establish the potential performance gains that adding radial stator vent airgaps may provide. A non-vented baseline case is used as a comparator against a range of designs, created using an automated optimisation algorithm, to select a new design with lower stator temperatures.

Electrical machines generate a range of losses removed via cooling. Increasingly more effort is being targeted on the thermal design of electrical machines as ever improving cooling analysis methods enable improvements in efficiency, life and power density [1].

In an air-cooled, through-ventilated, salient pole synchronous generator (SG) convection is the primary heat transfer mechanism utilised to remove the heat from component surfaces, with conduction a secondary mechanism. However, the thermal properties of electrical insulation materials impede conduction and where there is a long thermal path, for example in a long stator core, high local temperatures (hotspots) are typically seen. Therefore, it is common in larger machines to add radial vent airgaps between the stator laminations, to pass cooling air between the stator-casing cooling channel and the airgap. This brings the convective cooling air closer to the heat sources. Designing the placement, sizing and number of these vents is a highly complex and inter-disciplinary engineering problem, as a different split of air flow through the airgap, barrel gap or vent passages can cause a change in both the temperature and loss distribution. For this reason, approaches which are based on correlations cannot provide accurate predictions.

Lumped parameter thermal networks (LPTN) are based on simple analytical correlations and require calibration for every design change [1]. Thermal Finite Element Analysis (FEA) can only predict conduction with pre-set convective boundary conditions, which depend strongly on the vent design, and is therefore limited in the same way as LPTN [1]. Computational Fluid Dynamics (CFD) is the only modelling approach capable of predicting turbulent flow, convective and conductive heat transfer simultaneously. Hence, it has been chosen for the thermal modelling in this investigation.

However, CFD requires the external calculation of losses, which are used as inputs. As the analytical approaches used for the power losses determination are over-simplified, FEA is used in this paper to investigate the electromagnetic (EM) phenomena. Since stator vents are an inherently 3-D feature, 3-D FEA is often preferred to investigate their effects on the electromagnetic performance [2]. But a full 3-D analysis is computationally expensive. A synthesised 3-D FEA with approximated boundary conditions has been proposed by [3], with very positive results being achieved. Recently, a 2-D FEA of a 400 kVA salient-pole SG has shown excellent prediction results against experimental measurements [4]. In [4], appropriate compensation factors have been proposed to take the 3-D effects into account.

Most multi-physics models to date use LPTN for the thermal analysis. The use of CFD is not as common, due to its high computational effort and issues with coupling to an electromagnetic solver. Slupik et al. used CFD for the thermal analysis of a small 240 W DC motor [5]. The copper and iron losses were calculated using an analytical electromagnetic modelling software. Deeb investigated a 5 kW permanent magnet servo motor using a transient thermal FEA. CFD was used to determine the convective heat transfer coefficients required as input parameters. The EM performance was investigated by 2-D and 3-D FEA. Multiple cooling channel dimensions were optimised using a Goal Driven Optimization [6]. Zhang et al. used CFD to calculate the flow field around a

K. Bersch (kevin.bersch@nottingham.ac.uk), P. H. Connor (peter.connor@nottingham.ac.uk) and C. N. Eastwick (carol.eastwick@nottingham.ac.uk) are with the Fluids and Thermal Engineering Research Group. S. Nuzzo (stefano.nuzzo@nottingham.ac.uk) and G. Vakil (gaurang.vakil@nottingham.ac.uk) are with the Power Electronics, Machines and Control Research Group, all based within the Faculty of Engineering, University of Nottingham, Nottingham, UK.

M. Galea (michael.galea@nottingham.ac.uk) is with the University of Nottingham, UK and University of Nottingham Ningbo China, Ningbo, China.

R. Rolston (robert.rolston@cummins.com) is with Cummins Generator Technologies, Peterborough, UK.

200 kW asynchronous motor. The local velocities were used as input parameters for a coupled thermal and electromagnetic 3D-FEA [7]. The CFD model was highly simplified, for computational reasons, e.g. the motor endwindings were not modelled.

In this paper, the stator cooling of a synchronous generator is improved by venting the stator. Critical vent parameters, such as vent locations and widths, are optimised with the aim of reducing the machine hot spot located in the core stator windings. A Conjugate Heat Transfer CFD model is used for the thermal modelling. The parametric creation of geometry and mesh makes it possible to use automated optimisation algorithms, which require no additional user input after the initial model setup. The variation of copper and iron losses with the combined vent width is calculated using 2-D FEA. The electromagnetic losses are simplified down to correlations which have been implemented as input parameters for the thermal optimisation procedure.

II. Electromagnetic Modelling and Analysis

The previous section has highlighted how an accurate, combined electromagnetic and thermal analysis is necessary for a comprehensive understanding of the phenomena internally occurring in electrical machines. In particular, it is important to accurately estimate the power losses as these represent the direct link between the electromagnetic and the thermal aspects. Although this concept has general validity and is applicable to any type of electrical machine, in this paper the analysis is focused on a salient-pole, wound-field synchronous generator with a power rating of several hundred kVA.

This section highlights the major features of the FEA model of the SG and its experimental validation, with a focus on the losses. The validated model is then used and slightly modified to analyse the effects of radial stator vents on the overall machine losses.

A. The FEA model and its validation

Due to a number of reasons, the prediction of losses in electrical machines is a difficult task for electromagnetic designers. This is particularly true for the iron loss contribution for a number of reasons including:

1. The assumptions relative to the unidirectional nature of the fields inherently associated to the Epstein method [8] typically used to obtain the BH curve of the ferromagnetic materials.
2. The manufacturing aspects, which can significantly impact the magnetic properties of the materials.
3. Anomalous operating conditions.

However, a good level of confidence can be achieved from FEA models, which can provide very accurate values for the magnetic field and flux density in the various parts of the machine. Therefore, a 2-D FEA model of the investigated generator is built. The general details of such models and their validation are described in a number of works [9], [10] and are not reported here. However, the modelling aspects and validation relative to the copper and iron losses are described and presented in the next sections.

1) Copper losses

In physical devices, the voltage and current at the coils' terminals are not known directly, rather the way they are connected to external driving or load circuits. In Infolytica MagNet (the FEA-based software used in this paper), it is possible to couple the internal electromagnetic field quantities to the external electric circuit quantities by defining a circuit. A number of circuits equal to the number of windings composing the machine are coupled to the FEA model. These are the rotor field winding, the three-phase stator winding and the damper cage. One of the main limitations of a 2-D electromagnetic analysis is related to the fact the 3-D features of the SG are inherently neglected. However, to take these into account, a number of lumped resistances are considered in the model. In particular, the resistances of the rotor field and stator armature windings have been directly measured, experimentally, at the machine's terminals with an ohmmeter, thus allowing calibration and estimation of the additional resistances included in the FEA model to account for the end winding resistance values.

For the reasons above, 2-D transient analysis with motion evaluation can be used for accurately taking into account the most critical electromagnetic characteristics that relate to the end effects without resorting to the 3-D modelling. This is well proven by the comparison (at different loadings and power factors) between FEA and experimental copper losses, shown in Fig. 1, where the percentage error at full-load operation is equal to 0.5%. The values of the phase currents and resistances have been registered during the experimental tests at the thermal steady-state of the generator (i.e. at the machine operating temperature), permitting then to evaluate the copper loss contribution. In Fig. 1, the losses are shown p.u., where the experimental total (stator plus rotor) copper loss at full-load is used as base power.

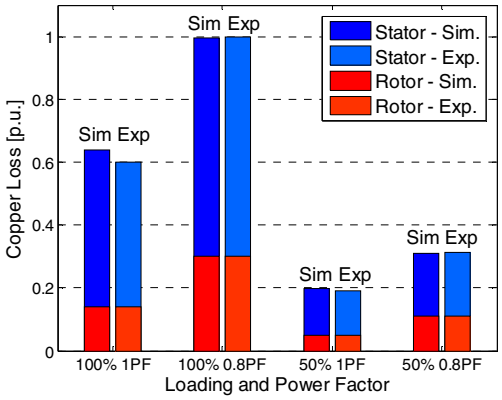

Fig. 1: Copper losses at different load levels and power factors: comparison between FEA and experimental results

2) Iron losses

As mentioned above, the iron loss determination is critical in synchronous generators, and electrical machines in general. Most FEA packages use the classical Steinmetz model [11], [12] to evaluate such loss contributions. This is the case of the software Infolytica MagNet which was used for the 2-D investigation. This may lead to very inaccurate results, particularly when high flux density harmonics are present. The method proposed here for the estimation of the iron loss in the SG studied is still based on Steinmetz equations, but extended

to all the harmonics [4]. The computational algorithm takes the magnetic field solution from a transient with motion 2-D FEA and extracts the flux-density waveforms corresponding to an electric cycle from the nodes of a grid built-on-purpose inside the iron regions, i.e. the stator and rotor steel. The Fourier series decomposition is then applied to these waveforms, considering the first 100 harmonics to account for the slotting harmonics. The Steinmetz equations extended to all the considered harmonic amplitudes are used to compute the hysteresis and eddy current loss components for every element delimited by the nodes of the customized grid. Finally, the total iron loss is calculated by summing the losses in each of the considered elements. The implemented algorithm considers the rotor surface losses, due to the slot harmonics, over the whole amount of iron loss.

From an experimental point of view, in SGs, core losses are historically measured at no-load and then assumed to be constant for all load levels and power factors. Also, only the total core loss is determined with no separation between rotor, stator or damper cage losses. In Fig. 2, the experimental iron loss value evaluated in such a way is compared with the SG losses calculated through the algorithm described above. The experimental iron loss value is used as base power to express the iron losses in p.u. In Fig. 2, it can be noticed that the assumption of having a constant iron loss with loading and power factor is not entirely true. Although they are of an ohmic-resistive nature, the damper cage losses are inherently included in the experimental iron loss value and therefore considered for the comparison. To be coherent with the experimental loss determination, the predicted and measured losses are compared only at no-load; a percentage error of approximately 10% is observed, highlighting the validity of the proposed computation algorithm.

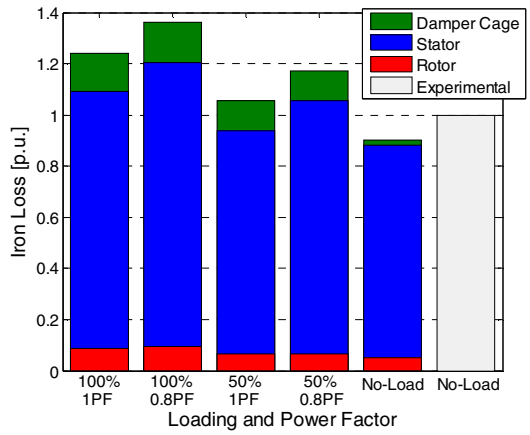

Fig. 2: Iron losses at different load levels and power factors: comparison between FEA and experimental results

B. The modified FEA model

In the previous section, the major features of the FEA model of the considered machine have been described. Special attention has been given to the copper and iron loss evaluation methods, as they represent the quantities which will be used in the CFD model described in the next section. These power loss sources have been compared against experimental measurements (see Fig. 1 and Fig. 2), confirming the validity of the built FE model.

Having validated the models, these can be safely used to analyse machines comprising stator ventilating ducts. As mentioned in section I. , the presence of such ventilation paths can improve the overall thermal behaviour of the machine, but at the cost of having less effective core length which in turns propagates less output power at the SG's terminals. Nevertheless, in traditional gensets, which typically use SG's similar to the type investigated in this paper, the voltage regulation system will compensate for a power drop by forcing an increased DC current value inside the rotor field winding. This comes with the drawback of increasing the rotor copper loss, which must be carefully considered, as it could contradict the main objective of the paper. The resulting trade-off study is undertaken as an integral part of the vent cooling optimisation study, presented in the second half of this paper. The validated FEA model has been used to evaluate copper and iron losses for a number of machine geometries with different ventilating duct widths, ranging from 10mm to 40mm, in steps of 5mm. Although the presence of such ducts is an inherently 3-D design feature and, therefore, a full 3-D FEA model would be the ideal platform for the analysis of the relevant phenomena, an equivalent length may be implemented in the 2-D model to take their effects into account. In fact, at the ventilating ducts, the flux density of the machine changes in the direction of the shaft. The flux density remains approximately constant over the length of the sheet core and presents a dip (i.e. decreasing and increasing gradually) over the axial length of the ventilating duct. Therefore, to take this field edge effect into account and the reduction of the effective core length, the equivalent axial length L_{eq} can be estimated by applying the classical Carter factor k_C [13]. This can be approximated by (1), where L is the total machine length (including core and ducts) and n_v and b_v are the number and the width of the ventilating ducts, respectively.

$$L_{eq} = L - k_c n_v b_v \qquad (1)$$

Considering all the aspects highlighted above and having implemented the equivalent length concept onto the 2-D FEA model, transient with motion simulations are performed to analyse the different machines at full-load operation. In order to achieve the same airgap flux density as the original machine, the field current is increased to compensate for the presence of the radial ducts, ensuring the same output power for all the investigated core lengths. This concept justifies the results shown in Fig. 3, where it can be observed how the rotor copper loss (evaluated at the expected steady-state operating temperature of the rotor) increases as the product $n_v b_v$ increases. In Fig. 3, both the copper loss (on the y-axis) and the total width of the ducts (on the x-axis) are expressed in p.u. of the rotor copper loss calculated for the existing machine and of the total machine length L, respectively. It can be also seen that at $n_v b_v = 0$, which refers to the original machine with no ventilating ducts, the rotor copper loss is at its minimum value, as expected. With respect to the rotor and stator iron losses (shown p.u. of the rotor and stator iron loss calculated for the original machine), a decreasing linear trend can be observed in Fig. 4, due to the fact that the removal of stator portions reduces the overall core volume, which is directly proportional to the iron losses.

The studies presented in this section represent a very important step in the design process at hand, as the copper and iron losses highlighted in Fig. 3 and Fig. 4 will be used as inputs for the set-up of the CFD model and the relevant optimisation strategy discussed in the second part of the paper.

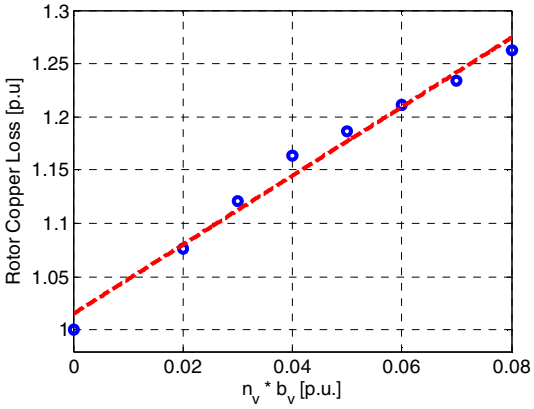

Fig. 3: Rotor copper loss trend vs. total width of ventilating ducts obtained via FEA simulations

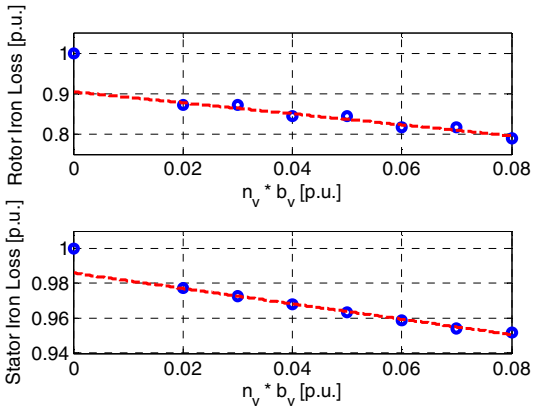

Fig. 4: Rotor and stator iron loss trend vs. total width of ventilating ducts obtained via FEA simulations

III. Thermal Modelling

A. Model setup

The model creation, solution and optimisation procedure all took place within ANSYS Workbench v17.2. The geometry and mesh were created using the DesignModeler and Meshing packages and subsequently solved with Fluent v17.2. The optimisation procedure was executed using the DesignXplorer feature. Combining all steps of the solution and optimisation process in one software package facilitates the creation of a model robust enough to handle the automatic updates during the optimisation process [14].

To predict fluid flow and heat transfer simultaneously, all solid parts and fluid zones inside the machine have been modelled. The machine is surrounded by a large cylindrical air domain which has boundaries that are sufficiently remote to not influence the flow around the SG. The cylinder boundaries are defined as a pressure outlet with a constant ambient backflow temperature. Due to the high complexity of the model, the SG was assumed to be 180° rotationally periodic, thus reducing computation time. This required some simplifications to the actual machine geometry. The flow through the investigated generator is driven by a 13 blade fan which had to be replaced by a 12 blade fan. Additionally, the location of one of the two inlets had to be moved circumferentially. However, early investigations and subsequent validation showed that these simplifications only have a negligible influence on the model accuracy (see section C. or [15]) . Fig. 5 shows the machine geometry created in ANSYS DesignModeler.

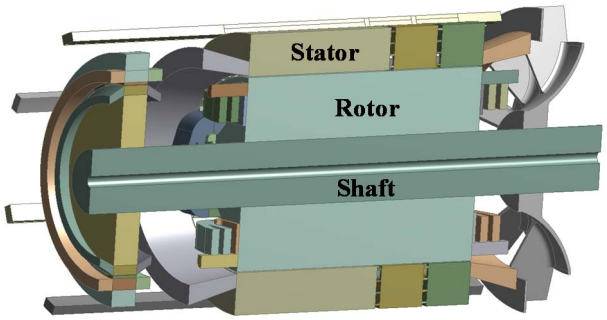

Fig. 5: Machine geometry; only solids shown for better visibility

Losses were implemented as a volumetric heat generation in Fluent. They were determined by experimental measurements and electromagnetic FEA (see section II.). Windage and friction, stray and stator copper losses were assumed to be constant in all configurations. The rotor copper, rotor and stator iron losses were varied with the combined vent width according to the correlations resulting from the EM FEA (see Fig. 3 and Fig. 4).

As windings are a combination of copper wires, resin and insulation material, the winding thermal conductivity perpendicular to the copper wire orientation is considerably lower compared to the conductivity in wire direction. The thermal conductivity in wire direction was assumed to be that of pure copper. The radial and tangential wire thermal conductivity was calculated according to the Hashin and Shtrikman approximation using the known thermal conductivity of copper and the insulation material. This approach has been used and validated by other researchers in the past [16], [17]. The change in copper wire orientation when the windings leave the core has been considered by varying the thermal conductivities using User Defined Functions (UDF) in Fluent.

Turbulence was modelled using the standard k-ε model with Enhanced Wall Treatment. It is commonly used for radial flux machines and has been validated for them by a number of researchers [18]–[20]. The SIMPLE algorithm is employed for the pressure-velocity coupling. The spatial discretisation of all variables is second order accurate. Rotation is implemented by the Multiple Reference Frame technique, which allows for a steady-state simulation despite the transient nature of the flow [21]. While it is less accurate than the fully transient Sliding Mesh approach, it is normally used for the analysis of electrical machines [19], [20], due to the much lower computational effort required.

All design points are initialised using the fully converged solution of one of the initially investigated cases. This reduces the number of iterations required to reach convergence. Only the airflow is solved for the first 900 iterations, as it requires more time to converge than the heat transfer, hence reducing computation time. Air flow and heat transfer are solved

simultaneously for the final 100 iterations. This resulted in a computation time of approximately 14 hours per design point (DP) on a desktop PC featuring a 3.5 GHz Intel Xeon Hexa-Core and 64 GB RAM. The mesh comprises of tetrahedral and hexahedral cells with an average cell count of 33.3 million.

B. *Optimisation Setup*

While it is theoretically possible to optimise a large number of input parameters simultaneously while considering multiple output parameters, the computational effort of CFD simulations limits the number of parameters to be varied in practice. In this case, it was feasible to optimise five input parameters simultaneously in the available timeframe. The machine hot spot in the investigated machine is located in the stator core windings. To increase machine lifetime, or increase the machine rating, minimising the peak stator temperature was set as the optimisation goal.

Early investigations showed that the addition of one vent is not sufficient for the targeted decrease in stator winding temperature, so a second vent was added to the geometry. Varying the number of vents during the optimisation was not feasible due to the model complexity and requirement for a robust model with a high quality mesh.

Adding a baffle to the stator-casing duct showed the potential to increase the flow rate through the vents hence reducing the stator winding temperatures. Locating the baffle at the rear axial surface of the first vent (from the inflow direction), protruding radially inwards from the casing, was determined to be the best location to reduce the peak stator winding temperature. Whilst the axial baffle location could be varied, it was not possible to implement this into the optimisation procedure due to time constraints. Thus the five parameters to be varied were:

- Axial location of the vents (2 parameters)
- Width of the vents (2 parameters)
- Radial length of the baffle (1 parameter)

The vent widths were limited to 1-4 % of the total core length for manufacturing reasons. The axial locations were restricted according to findings of initial investigations. Fig. 6 shows a schematic view of the generator core and the optimised parameters.

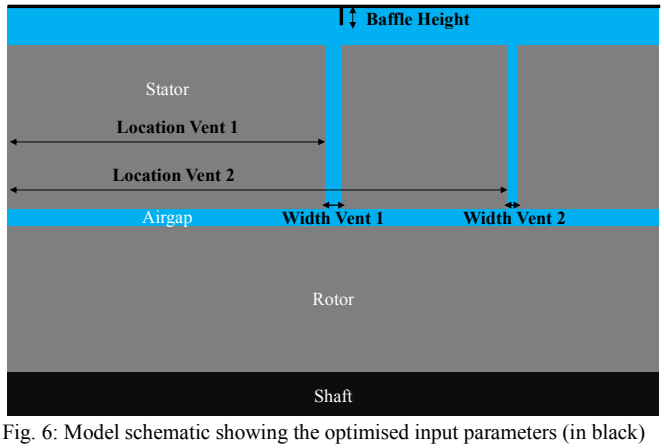

Fig. 6: Model schematic showing the optimised input parameters (in black)

A considerable number of variable input parameters had to be defined to make the geometry and mesh robust enough for the automatic updates during the optimisation procedure, and to vary the copper and stator iron losses with the combined vent width. The optimisation setup and methodology is based on the findings in [14]. The optimisation algorithm chosen for this investigation is the Adaptive Single-Objective method. It combines the creation of response surfaces based on Design of Experiments with a gradient-based optimisation algorithm, reducing the search domain until a converged solution is found. Further details about the optimisation setup and functionality of the algorithm can be found in [14] and [22].

C. *Experimental validation*

The CFD model of the non-vented machine has been validated experimentally by torque, mass flow and temperature measurements. Torque measurements were taken at 10-100 % synchronous speed. Mass flow measurements were taken at 30-100 % synchronous speed. The CFD torque is within 16 % of the measured data. CFD mass flow rates are within 13 % of the experimental data. The change in mass flow rate and torque with rotational speed is predicted correctly. Further details about the setup and results of the mass flow and torque validation can be found in [15].

During manufacture, PT100 RTDs were inserted into the rotor and stator windings. Steady-state temperature measurements were taken at full load. CFD rotor winding temperatures were within 12 % of the experimental data. CFD stator winding temperatures were within 13 % of the experimental data. The variation of temperature with core length is predicted correctly by the CFD model. Further details about the thermal validation will be published in future work.

IV. Results and Discussion

Due to time constraints, the optimisation algorithm was stopped manually after 14 days, before it reached convergence. At this point, 25 different stator ventilation configurations were evaluated and the parameter range narrowed down. The thermal performance of the best possible configuration found up to this point is analysed and compared to that of the benchmark machine.

The core length, vent location and vent width are normalised by dividing their axial length z through the total core length L (see (2)):

$$l^* = \frac{z}{L} \qquad (2)$$

The baffle height is normalised by dividing its radial height H through the total radial height of the stator barrel gap G (see (3)):

$$h^* = \frac{H}{G} \qquad (3)$$

Local temperatures T are normalised by dividing them through the peak temperature of the benchmark case $T_{max,B}$ (see (4)):

$$T_n = \frac{T}{T_{max,B}} \qquad (4)$$

Table 1 contains the vent parameters determined by the optimisation procedure as the best possible configuration:

Table 1: Optimal stator vent configuration (see (2) & (3))

Location 1st Vent	Location 2nd Vent	Width 1st Vent	Width 2nd Vent	Baffle Height
0.5 l^*	0.8 l^*	0.02 l^*	0.012 l^*	0.41 h^*

Fig. 7 shows the stator winding temperature profile over the core length for the benchmark and the vented machine. The temperatures were taken in the centre of the slot and averaged over all slots. The core end facing the inlet is located on the left of the graph. As the hot spot in the windings is located slightly off-centre, and the data is averaged over all slots, the peak normalised temperature of the benchmark machine in Fig. 7 only amounts to 0.95 $T_{max,B}$. In Fig. 8, the same comparison is shown for the rotor windings.

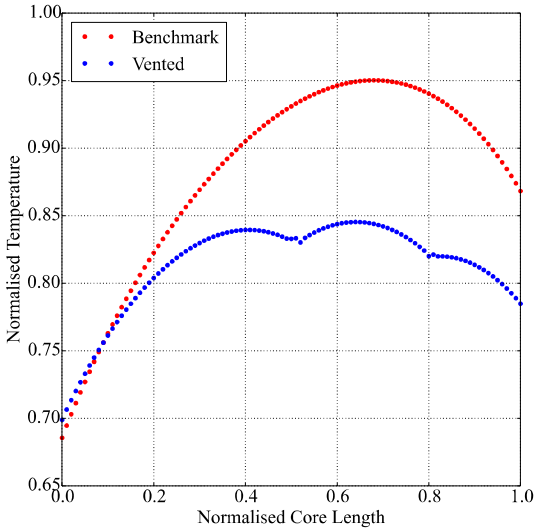

Fig. 7: Comparison of stator winding temperature profiles over the core length between benchmark and vented machine; obtained by CFD simulations

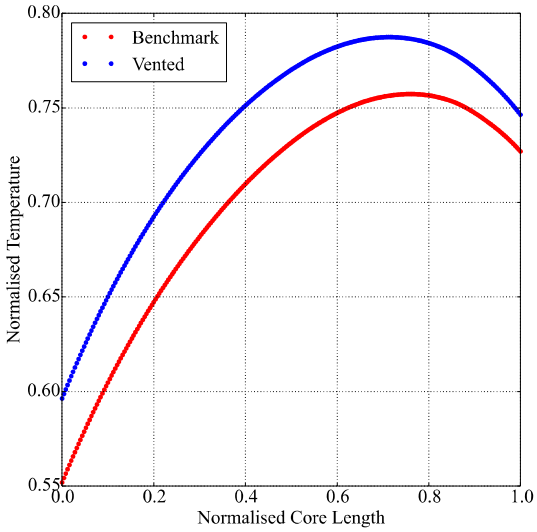

Fig. 8: Comparison of rotor winding temperature profiles over the core length between benchmark and vented machine; obtained by CFD simulations

The hot spot of the benchmark machine is located in the stator windings, approximately 70 % along the core length. From there, the winding temperature decreases steadily towards the core ends. It is 15 % higher at the side facing the outlet, as the surrounding air is considerably hotter at this end.

Fig. 7 clearly shows the positive impact venting the stator has on the stator winding temperatures. The peak temperature of the vented machine is reduced by 11.1 %, while the average temperature decreases 6.3 %. Up to 0.15 l^*, both configurations show almost the same thermal behaviour. From there one, the temperature gradient of the vented machine decreases in comparison to the benchmark one. A local temperature peak can be seen around 0.4 l^*. From here, the temperature decreases slightly until 0.5 l^*, the location of the first vent. The hot spot of the vented machine is located around 0.65 l^*.

The location of the two vents is evident by the two local minima at 0.5 l^* and 0.8 l^*. They are caused by the windings being directly cooled by the air flowing through the stator vents. By locating the vents on both sides of the benchmark machine hot spot, a fairly even temperature profile can be achieved. The temperature varies by less than 15 % between the inlet and outlet, in comparison to 25 % for the benchmark machine and is relatively constant for 0.3-0.8 l^*.

While the absolute rotor winding temperatures are lower in comparison to the stator windings (22 % on average for the benchmark machine), the rotor winding temperature profiles for both machines (see Fig. 8) are similar to the stator profile of the benchmark machine. Temperatures increase steadily from the core ends towards their peaks at 0.76 l^* (benchmark) and 0.71 l^* (vented) and are around 15 % higher on the core end facing the outlet. As the rotor current, and hence the rotor copper loss, is increased for the vented machine to compensate for the loss in active stator material, the rotor temperatures marginally increase in comparison to the benchmark case. The peak temperature increases by 1.8 %, while the average temperature rises 4.5 %.

Interestingly, venting the stator actually improves the rotor cooling. This was shown by running a simulation of the vented machine with the benchmark heat input. However, the improved rotor cooling is not sufficient to compensate for the increased rotor copper losses. The increase in rotor winding temperatures does not affect the lifetime of the vented machine though, as they are still below the stator winding temperatures.

It is worth noting that the presented methodology could be used to optimise for any goal the designer requires. For example, the technique could be used for minimising rotor temperatures if they are the concern for a particular design.

V. Conclusion

The cooling of an air-cooled, synchronous generator with a power rating of several hundred kVA has been improved by adding two radial vents to the stator and optimising critical vent parameters using a combined electromagnetic and thermal modelling approach. Initially, a 3-D Conjugate Heat Transfer CFD model of the original machine topology was created, predicting the fluid flow and thermal performance of the machine. Electromagnetic 2-D FEA was employed to determine the loss distribution within the machine. Both models were validated, showing good agreement with the experimental data.

The validated FEA model was modified and used to derive correlations between the combined vent width and rotor copper, rotor and stator iron losses. These correlations were implemented into a thermal optimisation procedure using a fully parametric model based on the validated CFD model. Five parameters: Vent locations, vent widths and height of a

baffle added to the stator-casing duct, were optimised simultaneously.

With the new design, the peak temperature of the investigated machine, located in the core stator windings, was reduced by 11.1 %, while the average stator winding temperature decreased by 6.3 %. A more uniform stator winding temperature profile was achieved. As venting the stator removes active stator material and the total core length was kept constant, the rotor current had to be increased to achieve the same power output. This increased the peak rotor winding temperature by 1.8 % and the average rotor winding temperature by 4.5 %, still keeping them below the stator winding temperatures. In future work, the increase in power density as a result of the design changes will be determined and the new machine design will be validated experimentally.

VI. Acknowledgment

The support of Cummins Generator Technologies for this research is gratefully acknowledged.

VII. References

[1] A. Boglietti, A. Cavagnino, D. Staton, M. Shanel, M. Mueller, and C. Mejuto, "Evolution and Modern Approaches for Thermal Analysis of Electrical Machines," *IEEE Trans. Ind. Electron.*, vol. 45, 2009.

[2] H. M. Hämäläinen, J. Pyrhönen, J. Nerg, and J. Puranen, "3-D finite element method analysis of additional load losses in the end region of permanent-magnet generators," *IEEE Trans. Magn.*, vol. 48, no. 8, pp. 2352–2357, 2012.

[3] W. Fei, P. C. K. Luk, D. Wu, and B. Xia, "Approximate three-dimensional finite element analysis of large permanent magnet sychronous generators with stator radial ventilating ducts," *IECON Proc. (Industrial Electron. Conf.*, pp. 7313–7318, 2013.

[4] S. Nuzzo, M. Degano, M. Galea, C. Gerada, D. Gerada, and N. Brown, "Improved Damper Cage Design for Salient-Pole Synchronous Generators," *IEEE Trans. Ind. Electron.*, vol. 64, no. 3, pp. 1958–1970, 2017.

[5] L. Slupik, J. Smolka, and L. Wrobel, "Experimentally validated numerical model of coupled flow, thermal and electromagnetic problem in small power electric motor," *Comput. Assist. Methods Eng. Sci.*, vol. 20, pp. 133–144, 2013.

[6] R. Deeb, "Thermal Calculation of Permanent Magnet Motors in High Current Technology," *Ph. D. Thesis*, 2013.

[7] Y. Zhang, J. Ruan, T. Huang, X. Yang, H. Zhu, and G. Yang, "Calculation of temperature rise in air-cooled induction motors through 3-d coupled electromagnetic fluid-dynamical and thermal finite-element analysis," *IEEE Trans. Magn.*, vol. 48, no. 2, pp. 1047–1050, 2012.

[8] IEC, "Magnetic materials - Part 2: Methods of measurement of the magnetic properties of electrical steel sheet and strip by means of an Epstein frame," vol. IEC 60404-, 2008.

[9] S. Nuzzo, S. Member, M. Galea, C. Gerada, S. Member, and N. Brown, "A Fast method for Modelling Skew and its Effects in Salient-Pole Synchronous Generators," *IEEE Trans. Ind. Electron.*, vol. 46, no. 10, pp. 7679–7688, 2017.

[10] C. Spagnolo, S. Nuzzo, G. Serra, C. Gerada, and M. Galea, "Analysis of salient-pole synchronous generators operating in single-phase condition," *Proc. - 2017 IEEE Work. Electr. Mach. Des. Control Diagnosis, WEMDCD 2017*, pp. 33–38, 2017.

[11] C. P. Steinmetz, "On the Law of Hysteresis," *Trans. Am. Inst. Electr. Eng.*, vol. 9, no. 1, pp. 1–64, 1892.

[12] C. P. Steinmetz, "On the Law of Hysteresis (Part II.) and Other Phenomena of the Magnetic Circuit," *Trans. Am. Inst. Electr. Eng.*, vol. 9, no. 1, pp. 619–758, 1892.

[13] J. Pyrhönen, T. Jokinen, and J. Hrabovcová, *Design of Rotating Electrical Machines*. Wiley, 2013.

[14] K. Bersch, P. H. Connor, C. N. Eastwick, M. Galea, and R. Rolston, "CFD Optimisation of the Thermal Design for a Vented Electrical Machine," in *Proc. - 2017 IEEE Work. Electr. Mach. Des. Control Diagnosis, WEMDCD 2017*, 2017, pp. 39–44.

[15] K. Bersch, P. H. Connor, C. N. Eastwick, and M. Galea, "A CFD and experimental investigation into a non-intrusive method for measuring cooling air mass flow rate through a synchronous generator," *9th Int. Conf. on Power Electronics, Machines and Drives (PEMD 2018)*, 2018.

[16] N. Simpson, R. Wrobel, and P. H. Mellor, "Estimation of equivalent thermal parameters of impregnated electrical windings," *IEEE Trans. Ind. Appl.*, vol. 49, no. 6, pp. 2505–2515, 2013.

[17] L. Idoughi, X. Mininger, F. Bouillault, L. Bernard, and E. Hoang, "Thermal model with winding homogenization and FIT discretization for stator slot," *IEEE Trans. Magn.*, vol. 47, no. 12, pp. 4822–4826, 2011.

[18] M. Shanel, "Investigation of Rotor Cooling in Salient Pole Electrical Machines," University of Nottingham, 2002.

[19] P. H. Connor, S. J. Pickering, C. Gerada, C. N. Eastwick, C. Micallef, and C. Tighe, "Computational fluid dynamics modelling of an entire synchronous generator for improved thermal management," *IET Electr. Power Appl.*, vol. 7, no. 3, pp. 231–236, 2013.

[20] S. J. Pickering, D. Lampard, J. Mugglestone, and M. Shanel, "Using CFD in the Design of Electric Motors and Generators," *Comput. Fluid Dyn. Pract.*, 2001.

[21] ANSYS Inc., "ANSYS FLUENT User's Guide v17.2," 2016.

[22] ANSYS Inc., "ANSYS DesignXplorer User's Guide v17.2," 2016.

VIII. Biographies

Kevin Bersch received a B.Sc. and M.Sc. degree in Mechanical Engineering and Business Administration from the RWTH Aachen University, Germany, in 2012 and 2015 respectively. He started his PhD in the Fluids and Thermal Engineering Research Group of the University of Nottingham in 2015. His research focusses on the thermal improvement of electrical machines using CFD and experimental investigations.

Stefano Nuzzo received his B.Sc. and M.Sc. in Electrical Engineering from the University of Pisa, Italy, in 2011 and 2014, respectively. He received his Ph.D. in electrical machines from the University of Nottingham, Nottingham, U.K, where he is currently working as a Research Fellow within the Power Electronics, Machines and Control (PEMC) Group. His current research interests are modelling, analysis and optimisation of salient-pole alternators and brushless excitation systems for industrial power generation application.

Peter H. Connor received an M.Eng. and Ph.D. from the Department of Mechanical, Materials and Manufacturing Engineering Department, University of Nottingham, UK, in 2009 and 2014 respectively. He is a Research Fellow in the Fluids and Thermal Engineering Research Group in the Faculty of Engineering at the University of Nottingham. His research interests are mechanical design and thermal management of electrical machines for industrial power generation and high-speed, high power-density aerospace applications.

Carol N. Eastwick received her BEng and PhD in Mechanical Engineering in 1990 and 1995 respectively. She is currently an Associate Professor in the Faculty of Engineering at the University of Nottingham, having worked on modelling and experimental investigations of thermofluids associated with rotating machinery for over twenty years.

Michael Galea received his PhD in electrical machines design from the University of Nottingham, UK, where he has also worked as a Research Fellow. He is currently the Deputy Director of the Institute for Aerospace Technology at the University of Nottingham, UK. He is also the Director of the Institute for Aerospace Technology at the University of Nottingham, Ningbo, China where he is also the Head of the Aerospace School. His main research interests are design, analysis and thermal management of electrical machines and drives, and electrification of aerospace systems.

Rob Rolston received his B.Sc. in Mechanical Engineering from the University of Bristol in 1978 and a Ph.D. from Queen's University of Belfast in 1984. During his career he has worked for GEC Mechanical Engineering Laboratory, United Biscuits Research and Technology Centre, EADS Astrium and for the last three years Cummins Generator Technologies. Areas of research and design include heat pumps, two-phase thermosyphon cooling systems, thermal modelling software, industrial ovens and burners, heat flux measurement systems, spacecraft thermal management and more recently alternator cooling systems.

Gaurang Vakil is an assistant professor within the electrical and electronics engineering department in the University of Nottingham